Composite Structures 255 (2021) 112902

Contents lists available at ScienceDirect

Composite Structures

journal homepage: www.elsevier.com/locate/compstruct

Size optimization method for controlling the buckling mode shape and critical buckling temperature of composite structures

Hoo Min Lee, Gil Ho Yoon *

Mechanical Engineering, Hanyang University, Republic of Korea

ARTICLE INFO

Keywords:
Size optimization
Buckling mode
Buckling temperature
Thermal buckling

ABSTRACT

The present study develops a novel size optimization method to control the buckling mode shape and associated buckling temperatures of plates. From a structural stability point of view, predicting the buckling temperature and mode shape of structures is one of the most important research topics in engineering. However, coming up with optimized engineering structures through engineering intuition for controlling these aspects is challenging. To address this limitation, the present study proposes the combination of finite element simulation and a size optimization scheme. Based on the idea that the structural buckling temperature and mode shape of a plate are mainly influenced by the thickness of the plate, in the optimization process, the thickness values of the divided sections of the target plate are set as the design variables. The buckling mode shape and buckling temperature are set as the objective functions, subjected to the total volume of the target plate. By applying the size optimization scheme, it is possible to determine the optimal thickness distributions for inducing the desired buckling mode shapes and buckling temperature values. The validity of the proposed size optimization method has been verified using several numerical examples.

1. Introduction

This study presents a novel structural optimization method by combining finite element simulation and a size optimization scheme to estimate, control and optimize the buckling mode shapes and buckling temperatures of plates in buckling cases caused by thermal expansion. From a structural stability perspective, predicting the buckling temperature and mode shapes of structures is vital in engineering. Parameters such as shape, thickness and geometric features can be optimized through mathematical programming to control the critical temperature and buckling mode shapes of structures. Before the optimization process, the influencing or dominant parameters should be pre-selected. Considering the simple thermal buckling theory, the present study sets the thickness values of homogeneous and composite plates as the design variables among several critical parameters in the size optimization process [1]. To demonstrate the effectiveness of the present optimization framework, several size optimization problems are solved considering the thermal buckling mode and buckling temperature.

The buckling of structures owing to thermal expansion has been a significant issue in various engineering problems [2,3]. Analyses on the buckling of composite materials to prevent such engineering problems and improve structural stability, can be found in [4,5]. Studies on the effect of temperatures on buckling [6–8], sudden changes of structure shapes under certain conditions [9–11], and differences between buckling due to thermal expansion and mechanical forces [12] have been conducted. Reviewing the relevant studies on the buckling phenomenon, various numerical and experimental methods have been developed and applied to solve buckling problems [13–15]. Despite the precedent research studies and increasing importance of structural optimization to control the buckling phenomenon, buckling related problems continue to be issues that are mainly solved by experience, intuition and empirical methods. Despite the limitations in solving the uncertainty of the buckling phenomenon, applications of the thermal buckling mode are emerging in structural optimization, to allow larger actuation for soft robots and develop 4D printing of flexible structures that are triggered by thermal loads [16,17]. Because the uncertainties in the buckling phenomenon still exist even with the increasing application demand, it is necessary to predict and control buckling problems. Therefore this study develops a size optimization scheme to control the buckling temperature and mode shape caused by thermal expansion.

The structural optimization scheme in the present study sets the thickness values of the structures as the design variables that mainly influence the buckling phenomena. To precisely control the tempera-

* Corresponding author at: School of Mechanical Engineering, Hanyang University, Seoul, Republic of Korea.
E-mail address: gilho.yoon@gmail.com (G.H. Yoon).

https://doi.org/10.1016/j.compstruct.2020.112902
Received 8 March 2020; Revised 23 June 2020; Accepted 26 August 2020
Available online 1 September 2020

tures and buckling modes of the structures, the present study optimizes the thickness values of the divided sections of the target structures. The buckling temperature and buckling modes are considered as the objective functions. To effectively control the buckling temperature, the objective function minimizing the differences between the buckling and reference temperatures is considered. To control the buckling mode, the objective function minimizing the buckling and target displacements is considered. The total volumes of the structures are set as the constraints using the dimensions as the design variables. To validate and illustrate the concept of the present study, homogeneous and composite structures mainly discretized by the shell element are considered [18–21]. The Eigen buckling simulation is carried out to compute the buckling temperature and buckling modes. For the optimization, the finite difference method (FDM) is used to compute sensitivity. With the developed optimization scheme, it is possible to optimize the buckling temperatures and buckling modes of homogeneous and composite structures. Several optimization problems are solved to verify the validity of the proposed scheme.

The present study is organized as follows: Section 2 presents the basic principle and equations for the thermal buckling analysis. Section 3 presents several size optimization formulations for controlling the buckling temperatures and buckling modes of homogeneous and composite structures which demonstrate the effectiveness and validity of the present study. The conclusions and future research topics are discussed in Section 4.

2. Optimization formulation

2.1. Linear eigen buckling analysis

Linear Eigen buckling is first formulated by defining the following stress–strain and strain–displacement relations [22],

$$\boldsymbol{\sigma} = D\boldsymbol{\varepsilon} \quad \boldsymbol{\varepsilon} = \mathbf{B}\mathbf{d} \tag{1}$$

where$\boldsymbol{\sigma}$, $\mathbf{D}$, $\boldsymbol{\varepsilon}$, $\mathbf{B}$ and $\mathbf{d}$ represent the stress vector, constitutive matrix, strain vector, strain–displacement matrix and displacement vector, respectively. The shell element composed of two-dimensional 4-node squared elements with six degrees of freedom per node is used for the Eigen buckling simulation.$\boldsymbol{\sigma}$, $\boldsymbol{\varepsilon}$ and $\mathbf{d}$ can be expressed as follows:

$$\begin{aligned} \boldsymbol{\sigma}^{\mathrm{T}} &= \{\sigma_x \ \sigma_y \ \sigma_z \ \tau_{xy} \ \tau_{yz} \ \tau_{zx}\} \quad \boldsymbol{\varepsilon}^{\mathrm{T}} = \{\varepsilon_x \ \varepsilon_y \ \varepsilon_z \ \gamma_{xy} \ \gamma_{yz} \ \gamma_{zx}\} \\ \mathbf{d}^{\mathrm{T}} &= \{u \ v \ w \ \theta_x \ \theta_y \ \theta_z\} \end{aligned} \tag{2}$$

The first three elements in each matrix represent the stress, strain and translational displacement in the x, y, and z coordinates, respectively. The next three elements represent the moment, plate curvature and rotational displacement in the x, y, z coordinates, respectively. Therefore, the system must consider both in-plane and bending conditions. The constitutive matrix is as follows:

$$\mathbf{D} = Et\begin{bmatrix} \bar{\mathbf{D}} & 0 \\ 0 & \frac{t^2}{12}\bar{\mathbf{D}} \end{bmatrix} \quad \bar{\mathbf{D}} = \begin{bmatrix} 1 & \nu & 0 \\ \nu & 1 & 0 \\ 0 & 0 & \frac{1-\nu}{2} \end{bmatrix} \tag{3}$$

where E, ν and t represent Young's Modulus, Poisson's ratio and the thickness of the shell element, respectively. Because 4-node mesh elements are used, their shape functions are as follows:

$$\begin{aligned} N_1 &= \frac{1}{4}(1-\xi)(1-\eta) \ \ N_2 = \frac{1}{4}(1+\xi)(1-\eta) \ \ N_3 = \frac{1}{4}(1+\xi)(1+\eta) \\ N_4 &= \frac{1}{4}(1-\xi)(1+\eta) \end{aligned} \tag{4}$$

The natural ξ-η coordinates in (4) are attached to the element with the origin at the center. The derivatives of these shape functions are used to formulate the strain–displacement matrix $\mathbf{B}$.

$$\mathbf{B} = \begin{bmatrix} \bar{\mathbf{B}} \\ \bar{\mathbf{B}} \end{bmatrix} \quad \bar{\mathbf{B}} = \begin{bmatrix} N_{1,\xi} & 0 & N_{2,\xi} & 0 & N_{3,\xi} & 0 & N_{4,\xi} & 0 \\ 0 & N_{1,\eta} & 0 & N_{2,\eta} & 0 & N_{3,\eta} & 0 & N_{4,\eta} \\ N_{1,\eta} & N_{1,\xi} & N_{2,\eta} & N_{2,\xi} & N_{3,\eta} & N_{3,\xi} & N_{4,\eta} & N_{4,\xi} \end{bmatrix} \tag{5}$$

The strain–displacement matrix $\mathbf{B}$ is used to calculate the element physical stiffness matrix of single shell layer $\mathbf{K}_o$ based on the Kirchhoff plate formulation [23]. The constitutive matrix is denoted by $\mathbf{D}$. The element physical stiffness matrix of composite shell $\mathbf{K}_{o,c}$ is calculated as the sum of layer stiffnesses over the total number of layers, L [24].

$$\mathbf{K}_o = \int_V \mathbf{B}^{\mathrm{T}}\mathbf{D}\mathbf{B}\,\mathrm{d}V \tag{6}$$

$$\mathbf{K}_{o,c} = \sum_{l=1}^{L}\int_V \mathbf{B}_l^{\mathrm{T}}\mathbf{D}_l\mathbf{B}_l\mathrm{d}V \tag{7}$$

The displacement $\mathbf{U}$ is computed as follows:

$$\mathbf{U} = (\mathbf{K}_{o,c})^{-1}\mathbf{F} \tag{8}$$

The static deformation vector, $\mathbf{U}$ is used to calculate the stresses. The stress values are evaluated at a discrete set of Gauss points. The $\mathbf{G}$ and $\mathbf{S}$ matrices are computed as follows:

$$\mathbf{G} = \begin{bmatrix} N_{1,\xi} & 0 & N_{2,\xi} & 0 & N_{3,\xi} & 0 & N_{4,\xi} & 0 \\ N_{1,\eta} & 0 & N_{2,\eta} & 0 & N_{3,\eta} & 0 & N_{4,\eta} & 0 \\ 0 & N_{1,\xi} & 0 & N_{2,\xi} & 0 & N_{3,\xi} & 0 & N_{4,\xi} \\ 0 & N_{1,\eta} & 0 & N_{2,\eta} & 0 & N_{3,\eta} & 0 & N_{4,\eta} \end{bmatrix} \tag{9}$$

$$\mathbf{S} = \begin{bmatrix} \boldsymbol{\sigma}_{xx} & \boldsymbol{\sigma}_{xy} & 0 & 0 \\ \boldsymbol{\sigma}_{xy} & \boldsymbol{\sigma}_{yy} & 0 & 0 \\ 0 & 0 & \boldsymbol{\sigma}_{xx} & \boldsymbol{\sigma}_{xy} \\ 0 & 0 & \boldsymbol{\sigma}_{xy} & \boldsymbol{\sigma}_{yy} \end{bmatrix} \tag{10}$$

The element geometric stiffness matrix of single shell layer $\mathbf{K}_\sigma$ is calculated using the $\mathbf{G}$ and $\mathbf{S}$ matrices. Similar to the element physical stiffness matrix of the single shell, the element geometric stiffness matrix of composite shell $\mathbf{K}_{\sigma,c}$ is also calculated as the sum of layer stiffnesses over the total number of layers, L.

$$\mathbf{K}_\sigma = \int_V \mathbf{G}^{\mathrm{T}}\mathbf{S}\mathbf{G}\,\mathrm{d}V \tag{11}$$

$$\mathbf{K}_{\sigma,c} = \sum_{l=1}^{L}\int_V \mathbf{G}_l^{\mathrm{T}}\mathbf{S}_l\mathbf{G}_l\mathrm{d}V \tag{12}$$

Using the calculated figures, it is possible to establish the Eigen buckling formulation of the shell elements.

$$[\mathbf{K}_{o,c} + \lambda_{cr}\mathbf{K}_{\sigma,c}]\,\mathbf{v} = 0 \tag{13}$$

Eigen buckling occurs because of the load $\mathbf{F}$ applied to the structure at (8). From the formulation, Eigenvalues λ_{cr} are the load multipliers that scale the load vector to critical values that cause buckling. Eigenvectors $\mathbf{v}$ are the buckling shapes associated with the corresponding loads.

2.2. Optimization formulation

As stated in the introduction, the present study divides the shell structure into N sections and sets the thicknesses of the sections as the design variables. To control the buckling temperature, the following optimization formulation is considered.

$$\begin{aligned} \text{OP1}: \ \underset{t}{\text{Min}} \ f_{obj} &= \sum_{k=1}^{n}\left(T_{critical,k} - T_{objective,k}\right)^2 \\ \text{Subject, to} \ \sum_{i=1}^{N} a_i t_i &\leqslant V^* \\ t_{min} \leqslant t_i \leqslant t_{max}\,, \ i &= 1 \ldots N \ \text{sections} \end{aligned} \tag{14}$$

where the buckling temperature of the k-th buckling mode, and the reference temperature are denoted by $T_{critical,k}$ and $T_{objective,k}$, respectively. The upper and lower bounds of the design variable are denoted by t_{max} and t_{min}, respectively. The number of the considered temperatures is n. The area of the section and thickness (the design variable) are denoted by a_i and t_i, respectively. The upper bound of the allowable volume is V^*. The buckling mode shapes are optimized as the second optimization problem, using the following optimization formulation.

$$\begin{aligned} \text{OP2}: \ \min_{t} f_{obj} &= \sum_{k=1}^{n} \left(\delta_{critical,k} - \delta_{objective,k}\right)^2 \\ \text{Subject, to} \ &\sum_{i=1}^{N} a_i t_i \leqslant V^* \\ t_{min} \leqslant t_i \leqslant t_{max}&, \ i = 1 \ldots N \text{ sections} \end{aligned} \tag{15}$$

where the displacements of the target points and target displacements of the k-th Eigenmode are $\delta_{critical,k}$ and $\delta_{objective,k}$, respectively.

The buckling and associated sensitivity analyses based on the FDM are carried out after formulating the above optimization formulations. The forward buckling analysis is performed using the thermal load on the structures. The corresponding Eigenvalue is multiplied with the thermal load results in the buckling temperature in the objective function. The developed optimization process is shown in Fig. 1. To verify the validity of the proposed optimization formulation, several structures with both homogeneous and composite material properties are considered.

3. Optimization results

This section presents several optimization examples to verify the validity of the proposed formulations. The MATLAB optimizer, fmincon, is used to solve the optimization problems; the structural analysis is carried out using ANSYS APDL (Shell 63 for the homogenous structure and Shell 181 for the composite structure).

3.1. Example 1: Controlling buckling temperature of homogeneous plate

Fig. 2 shows the first optimization example with a homogenous material. The analysis domain is a 100 mm by 10 mm steel plate fixed at both ends. Young's modulus, Poisson's ratio and the thermal expansion coefficient are set to 200 GPa, 0.3 and $11.7 \times 10^{-6}\,^{\circ}\text{C}^{-1}$, respectively.

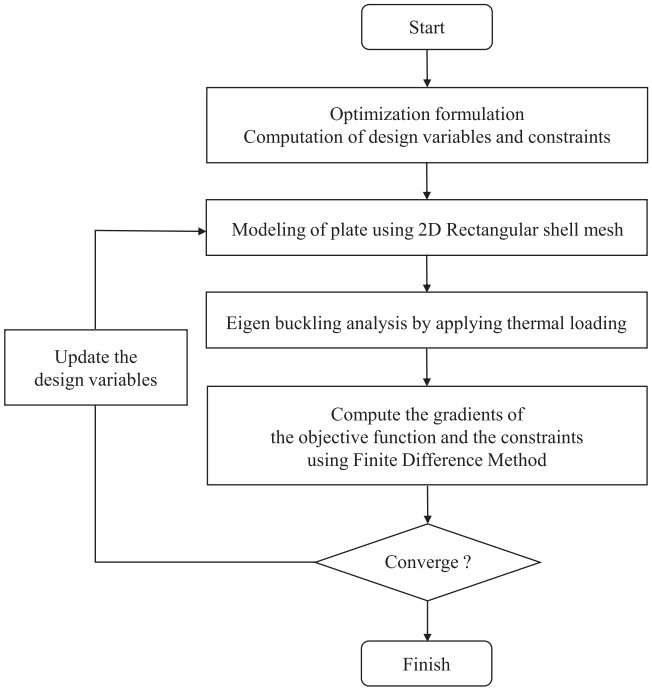

Fig. 1. Flow chart of the optimization procedure to control buckling temperature and buckling mode shape.

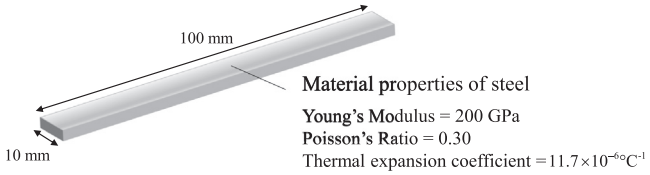

Fig. 2. Material properties of homogeneous plate.

For the optimization, the plate in Fig. 2 is divided into 25 even areas with lengths and widths of 20 mm and 2 mm, respectively. The initial thickness values of the sections are set as 1 mm. The first three buckling temperature values are initially 28.3176 °C, 58.0481 °C and 114.2040 °C, with uniform thicknesses of 1 mm, respectively. For the first example, the target buckling temperatures in the optimization problem, OP1, are set as 55 °C, 85 °C and 165°C, respectively. The thickness values of each of the divided areas are set as the design variables and vary from 0.1 mm to 2.0 mm. Because the structural optimization problem has a few design variables, the sensitivity computation of the objective functions using the FDM is straight forward and efficient, not requiring the derivation of the adjoint sensitivity analysis. To demonstrate this, Fig. 3 shows the results of the sensitivity analysis depending on the perturbation size. The seven arbitrarily chosen design variables are perturbated with $\Delta t = 0.01$, $\Delta t = 0.001$, and $\Delta t = 0.0001$ to demonstrate the accuracy. This shows that the sensitivity of the present FDM scheme is accurate from a computation point of view. In our numerical implementation, the perturbation step is set to 0.001 based on the accuracy of the computation. The optimized results of this example for controlling the buckling temperature values are shown in Fig. 4.

The optimization results in Fig. 4 show that the first three optimized buckling temperatures are converged to the target buckling temperatures of 55°C, 85°C and 165°C, respectively. The discrepancies of the buckling temperatures of the optimized structure in Fig. 4(c) to the target temperatures are less than 0.1%. This example shows that the proposed optimization formulation can be used to obtain the optimized thickness of a homogeneous plate.

3.2. Example 2: Controlling buckling temperature of composite plate

For the second example, an optimization problem controlling the buckling temperature of a structure with composite material as shown

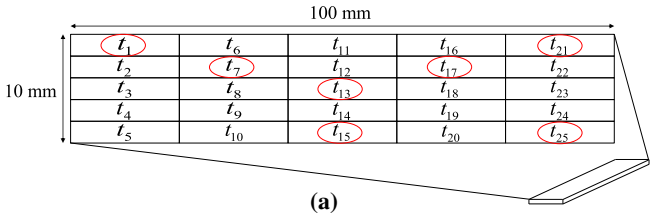

(a)

Design Variable	Sensitivity with $\Delta t = 0.01$	Sensitivity with $\Delta t = 0.001$	Sensitivity with $\Delta t = 0.0001$
t_1	3.1112	3.0802	3.0771
t_7	0.1801	0.1745	0.1740
t_{13}	4.8346	4.7997	4.7961
t_{15}	4.9079	4.8767	4.8735
t_{17}	0.1801	0.1745	0.1740
t_{21}	3.1112	3.0802	3.0771
t_{25}	3.1112	3.0802	3.0771

(b)

Fig. 3. (a) Illustration of the design variables and (b) FDM tests with the perturbations.

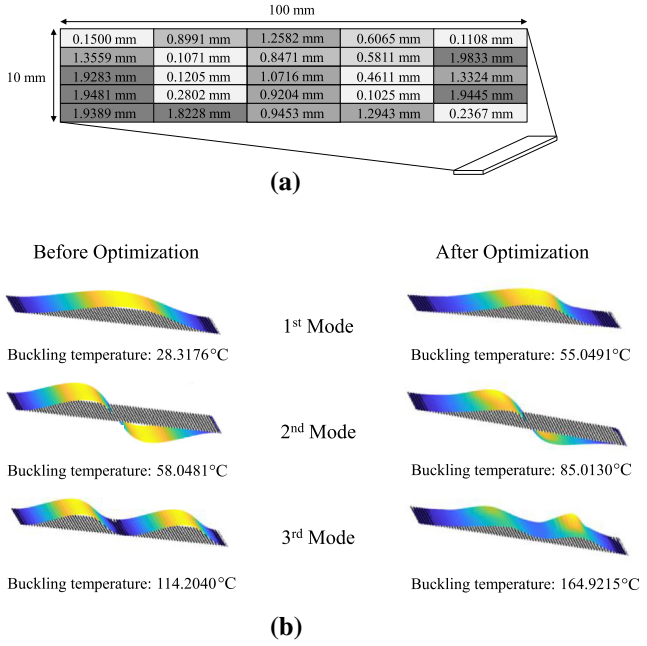

	First mode buckling temperature (°C)	Second mode buckling temperature (°C)	Third mode buckling temperature (°C)
Target	55.0000	85.0000	165.0000
Result	55.0491	85.0130	164.9215
Error	0.0893%	0.0153%	0.0476%

(c)

Fig. 4. (a) Optimized layout, (b) first three mode shapes before and after optimization, and (c) analysis of the optimization results.

in Fig. 5 is considered. The analysis domain is 100 mm by 10 mm with fixed ends. The material properties assigned to the first and second materials are those of steel and copper, respectively.

In this example, the plate is also divided into 25 even sections with the same initial thickness of 1 mm with a range between 0.1 mm and 2 mm. The initial buckling temperature values of the initial designs are 28.2600 °C, 57.9040 °C and 113.8100 °C, respectively, for the first three buckling modes. For illustration purposes, it is assumed that the thickness values of steel and copper at each section are identical $(t_{i,copper} = t_{i,steel} = t_i/2, i = 1, \ldots, N)$. For example, if the design variable which can be interpreted as the sum of the thickness values of copper and steel, is 1 mm, the thicknesses of steel and copper are each 0.5 mm; the ratio of the thicknesses is fixed. With this pre-assumption, OP1 is solved using an optimization algorithm with target temperatures of 55°C, 85°C and 165°C. The optimized thickness distribution, its buckling temperature and buckling mode are shown in Fig. 6. As in the first example, the optimizer can be used to obtain the optimized thickness distribution, successfully minimizing the gap between the target and buckling temperatures for engineering purposes .

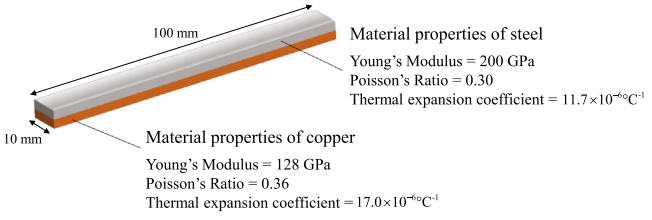

Fig. 5. Material properties of composite plate.

The differences in the homogeneous and composite plates are expected owing to the differences in the stiffness, thermal buckling temperature and thermal buckling mode. To comply with the target buckling temperatures, the thickness values of the plates are modified to find the optimum thickness distributions. It should be noted that the target buckling temperatures in Figs. 4 and 6 are identical and the material models are different. By comparing the optimization results, it can be referred that the thicker sections in the optimized design of the homogeneous material are positioned on the bottom left and right side of the plate, where t_3, t_4, t_5, t_{10}, t_{22}, and t_{24} have greater values compared to the rest of the design variables. The thicker sections in the optimized design of the composite material are positioned relatively at the center of the plate, where t_3, t_5, t_6, t_{11}, t_{12}, t_{14}, t_{15}, t_{16}, t_{20}, and t_{21}, have greater values compared to the rest of the design variables.

The differences in the thickness distribution cause a difference in the mode shapes of both plates. Unsymmetrical designs can be obtained for the both homogeneous and composite plates, to satisfy the target buckling temperatures. Both plates show unsymmetrical mode shapes, whose asymmetricity becomes more deteriorated with increasing mode numbers. However, there is a difference in the points where the plates show the greatest out-of-plane displacement. In terms of the second and third mode, the greatest displacement of the homogeneous plate is at the section with design variable t_{16}, whereas that of the composite plate is at the section with design variable t_{20}. The difference in thickness distribution causes a difference in sensitivities to thermal loads for each section, resulting in different mode shapes for the homogeneous and composite plates despite the similar buckling temperature values. By evaluating the mode shapes of the designs in

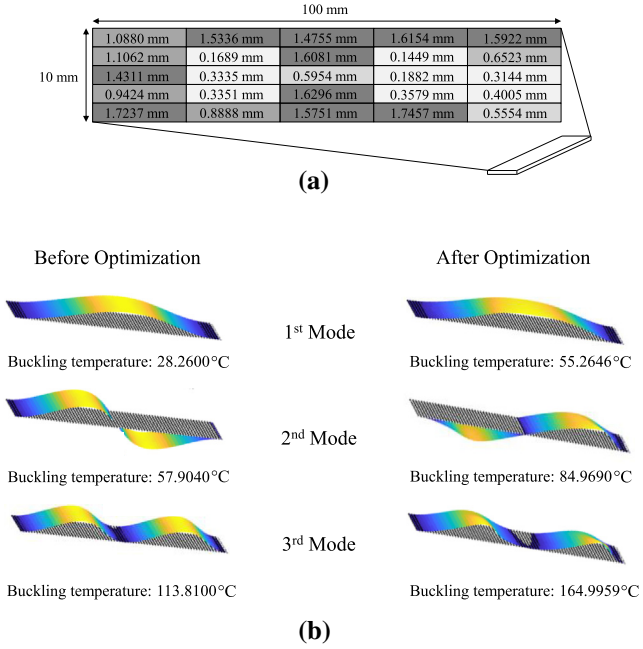

	First mode buckling temperature (°C)	Second mode buckling temperature (°C)	Third mode buckling temperature (°C)
Target	55.0000	85.0000	165.0000
Result	55.2646	84.9690	164.9959
Error	0.4811%	0.0365%	0.0025%

(c)

Fig. 6. (a) Optimized layout, (b) first three mode shapes before and after optimization, and (c) analysis of the optimization results.

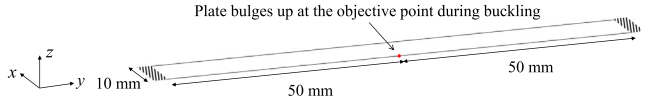

Fig. 7. Optimization problem maximizing the z-displacement of the target point.

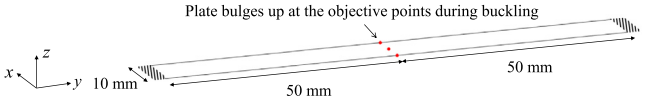

Fig. 9. Optimization problem maximizing the z-displacement of the target points.

Figs. 4 and 6, the optimization algorithm identifies the designs that are difficult to find by engineered intuition. It should be noted that it is not possible to obtain optimized results using some arbitrarily chosen buckling temperatures or non-physical temperature values.

3.3. Example 3: Controlling buckling mode shape of composite plate

For the next example, the buckling mode shape of a composite plate is considered. The composite material model is similar to that in the second example in Fig. 5. As in the previous examples, the initial thickness values are set as 1 mm and range between 0.1 mm and 2 mm. In this example, a single point at the side of the center of the design domain is chosen as the target point, as shown in Fig. 7. The aim is to identify an optimized layout that makes the plate bulge up during buckling by maximizing the z-displacement of the target point.

The optimization, OP2, is carried out on the composite material. Fig. 8 shows the optimized layout and its first buckling mode. As illustrated, the optimized design and buckling mode are symmetrical. It is interesting that the mode of the section containing the target point and the three adjacent sections is 0.1000 mm, whereas the last section is relatively stiffer with 1.7193 mm. It should be noted that it is also difficult for engineers to imagine this design; the present study can identify a locally optimized layout.

The above example illustrates that the present optimization algorithm can be used to determine an optimized layout controlling the buckling mode as well. To further test the validity of the proposed size optimization scheme, the displacements of the additional points at the center line are included in Fig. 9. This is done to identify an optimized layout that would force the simultaneous movement of the center line during buckling.

With the present optimization formulation, the optimized thickness distribution in Fig. 10(a) can be obtained. As illustrated in Fig. 10(b), the symmetric mode shape is obtained to satisfy the objective function.

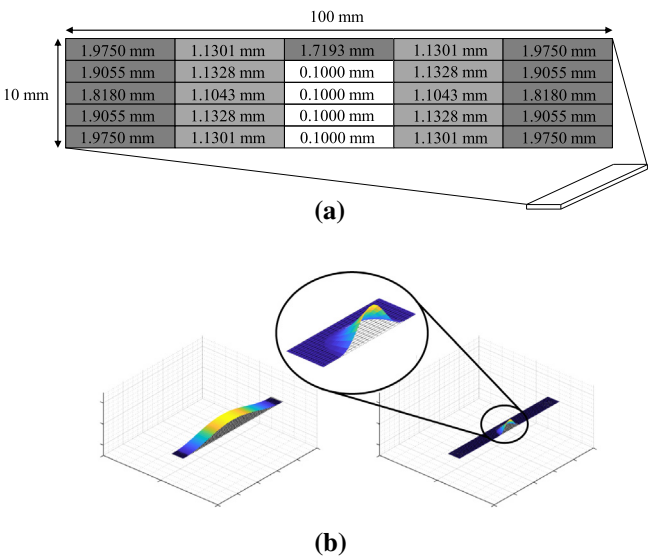

Fig. 8. (a) Optimized layout and **(b)** first mode before and after optimization.

It should be noted that the Eigenmodes are normalized by the mass matrix.

To further investigate the present optimization, the analysis domain is divided into smaller sections with lengths and widths of 10 mm and 1 mm, respectively; to consider the displacements of the points marked in Fig. 11(a), the design variables are set to range between 0.1 mm and 5.0 mm. The aim of this optimization problem is to determine an optimized layout minimizing the gap between the target mode in Fig. 11(b) and the buckling mode. Fig. 12(a) and 12 (b) show the corresponding design and optimized modes. This example also illustrates that the proposed optimization scheme can be used to identify an optimized layout to manipulate the buckling mode.

3.4. Example 4: Controlling buckling mode shape of composite structure

For the final example, Figs. 13 and 14 show the definition of the optimization problem on the composite material (steel and copper), and the optimized layout, respectively. The objective of this optimization problem is to make the buckling mode of the structure resemble a gripper. To achieve this, the objective displacements for the displacements of the points marked in Fig. 13(a), are set as shown in Fig. 13 (b). The size of each finger is 45 mm by 10 mm and the center rectangular domain is 10 mm by 10 mm. The design domain is divided into 101 sections. The number of divisions in each finger is 25 and each divided section has a length and width of 9 mm and 2 mm, respectively. The initial thickness of each fingers is set to 1 mm, and that of the center domain is set to 3 mm. The design variables are set to range between 0.1 mm and 2 mm. Fig. 14(a) shows the optimized layout, Fig. 14(b) shows the mode shape and Fig. 14(c) shows the optimized displacement values of the optimized structure. This example illustrates the potential application of the present optimization algorithm in soft robots.

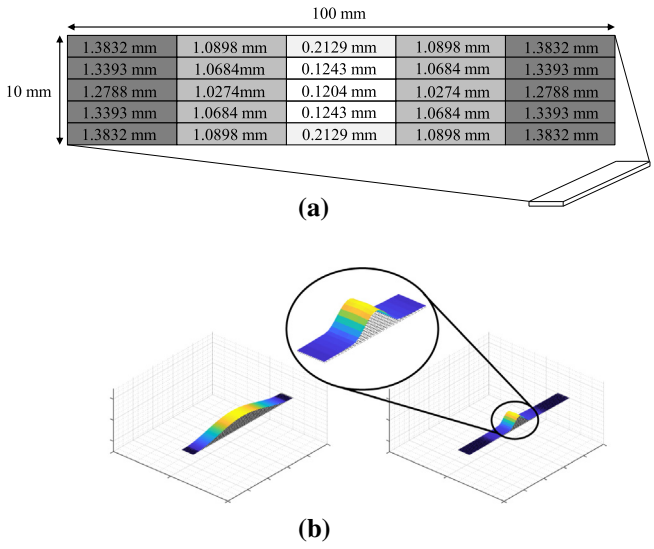

Fig. 10. (a) Optimized layout and (b) first mode before and after optimization.

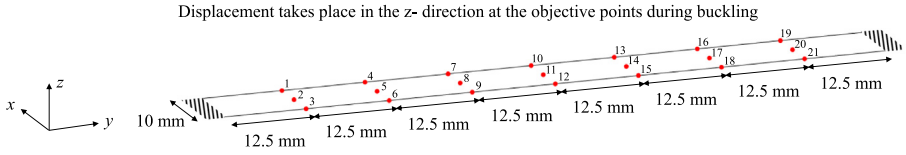

(a)

Objective point numbers	1 2 3	4 5 6	7 8 9	10 11 12	13 14 15	16 17 18	19 20 21
Objective displacement values (mm)	0.3000	0.6000	0.9000	0.0000	-0.9000	-0.6000	-0.3000

(b)

Fig. 11. (a) Objective points of the plate for the control of displacement values and **(b)** assigned displacement values for each objective point.

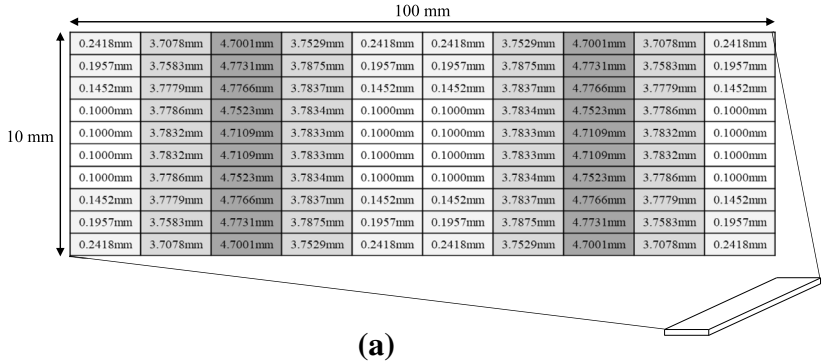

(a)

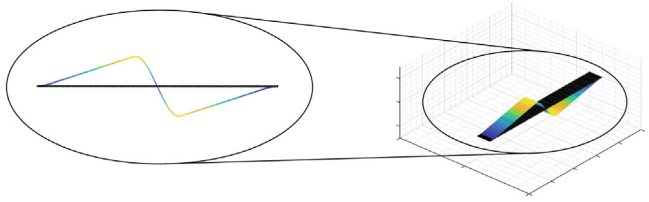

(b)

Objective point numbers	1 2 3	4 5 6	7 8 9	10 11 12	13 14 15	16 17 18	19 20 21
Resultant displacement values (mm)	0.2440	0.5790	0.9140	0.0000	-0.9140	-0.5790	-0.2440

(c)

Fig. 12. (a) O**ptimized layout,** (b) **first mode shape after optimization, and** (c) **resultant displacement values of the objective points.**

4. Conclusion

This study presents several size optimization formulations for controlling the buckling mode and buckling temperature of homogenous and composite plates. It is important to control the thermal induced buckling phenomenon because it can cause unanticipated issues such as fatigue failure, noise and delamination. These issues can be avoided by preventing or controlling the temperature distribution in structures. The thermal buckling temperature and thermal buckling mode can be numerically and accurately analyzed with the help of computational

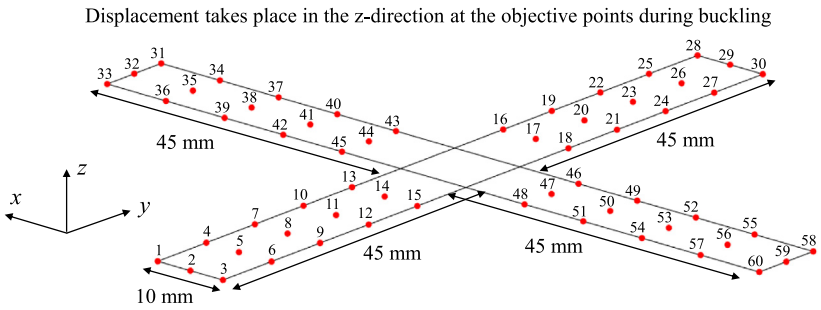

(a)

Objective point numbers	1 2 3	4 5 6	25 26 27	28 29 30	31 32 33	34 35 36	55 56 57	58 59 60
Objective displacement values (mm)	1.0000	0.4000	0.4000	1.0000	1.0000	0.4000	0.4000	1.0000

(b)

Fig. 13. (a) **Optimization problem definition and** (b) **target displacements.**

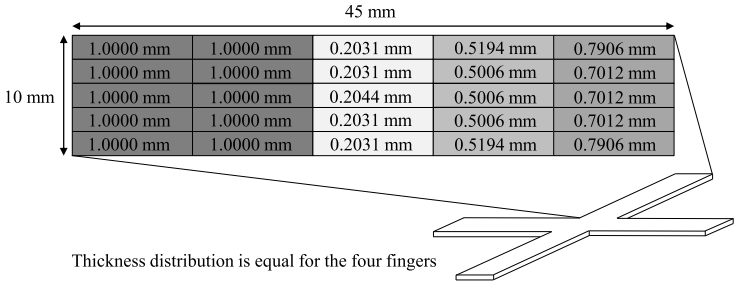

(a)

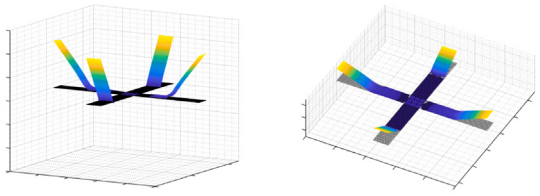

(b)

Objective point numbers	1 2 3	4 5 6	25 26 27	28 29 30	31 32 33	34 35 36	55 56 57	58 59 60
Resultant displacement values (mm)	0.9180	0.4220	0.4220	0.9180	0.9180	0.4220	0.4220	0.9180

(c)

Fig. 14. **(a)** Optimized layout, **(b)** first mode shape after optimization and **(c)** resultant displacement values of the objective points.

theories. Additionally, it is possible to apply the optimization framework using mathematical programming to maximize, minimize or prescribe the buckling temperature or buckling mode. To validate and illustrate these approaches, the present study considered homogeneous and composite structures and formulated several structural optimization problems whose design variables were the thickness values of the plates. Using these optimization formulations, it was possible to determine optimal thickness distributions which comply with the tar-

get thermal buckling mode as well as the target buckling temperature. It was also observed that the present optimization framework could be applied to optimize the performance of soft robots or 4D printing of flexible structures. In conclusion, the present study presented and validated several optimization frameworks for controlling the thermal buckling mode and thermal buckling temperature.

Declaration of Competing Interest

The authors declare that they have no known competing financial interests or personal relationships that could have appeared to influence the work reported in this paper.

Acknowledgments

This work was supported by the National Research Foundation of Korea (NRF) grant funded by the Korea government (MSIT) (No. 2018R1A5A7025522) and the research fund of Institute of Civil Military Technology Cooperation of Korea (No. UM16201RD2).

References

[1] Jenkins JM, Sefic WJ. Experimental investigation of thermal-buckling characteristics of flanged, thin-shell leading edges. Natl Aeronaut Space Admin Edwards 1966.
[2] Bai J, Xiong J. Temperature effect on buckling properties of ultra-thin-walled lenticular collapsible composite tube subjected to axial compression. Chin J Aeronaut 2014;27:1312–7.
[3] Fu T, Chen Z, Yu H, Li C, Zhao Y. Thermal buckling and sound radiation behavior of truss core sandwich panel resting on elastic foundation. Int J Mech Sci 2019;161:1050–5.
[4] Chai H, Babcock C. Two-dimensional modelling of compressive failure in delaminated laminates. J Compos Mater 1985;19:67–98.
[5] Yufeng X, Wei X. Analytical solution methods for eigenbuckling of symmetric cross-ply composite laminates. Chin J Aeronaut 2017;30:282–91.
[6] Moulin D, Combescure A, Acker D. A review of thermal buckling analysis methods. Nucl Eng Des 1989;116:255–63.
[7] Rakow JF, Waas AM. Thermal buckling of metal foam sandwich panels for convective thermal protection systems. J Spacecraft Rockets 2005;42:832–44.
[8] George N, Jeyaraj P. Nonuniform heat effects on buckling of laminated composite beam: experimental investigations. Int J Struct Stab Dyn 2018;18 Article 1850153.
[9] Orthwein WC. Thermal buckling of a bimetallic strip. J Vib Acoust 1984:538–42.
[10] Yan Z, Zhang F, Wang J, Liu F, Guo X, Nan K, et al. Controlled mechanical buckling for origami-inspired construction of 3D microstructures in advanced materials. Adv Funct Mater 2016;26:2629–39.
[11] Cui J, Adams J, Zhu Y. Pop-up assembly of 3D structures actuated by heat shrinkable polymers. Smart Mater Struct 2017;26:125011.
[12] Saha S, Ali A. Thermal buckling and postbuckling characteristics of extensional slender elastic rods. J Mech Eng 2009;40:1–8.
[13] Wu C, Fang J, Li Q. Multi-material topology optimization for thermal buckling criteria. Comput Methods Appl Mech Eng 2019;346:1136–55.
[14] Zhao W, Singh K, Kapania RK. Thermal buckling analysis and optimization of curvilinearly stiffened plates with variable angle tow laminates. J Spacecraft Rockets 2019;56:1189–204.
[15] Dong X, Ding X, Li G, Lewis GP. Stiffener layout optimization of plate and shell structures for buckling problem by adaptive growth method. Struct Multidisc Optim 2020;61:301–18.
[16] Cheng NG, Gopinath A, Wang L, Iagnemma K, Hosoi AE. Thermally tunable, self-healing composites for soft robotic applications. Macromol Mater Eng 2014;299:1279–84.
[17] Ly ST, Kim JY. 4D printing–fused deposition modeling printing with thermal-responsive shape memory polymers. Int J Precis Eng Manuf-Green Technol 2017;4:267–72.
[18] Bala P, Rathinam N, Srinivasan R. Finite element analysis of buckling of thin cylindrical shell subjected to uniform external pressure. J Solid Mech 2009;1:148–58.
[19] Yang Q. Simplified approaches to buckling of composite plates [Master Thesis]. Universitetet i Oslo; 2009.
[20] Xu F, Abdelmoula R, Potier-Ferry M. On the buckling and post-buckling of core-shell cylinders under thermal loading. Int J Solids Struct 2017;126:17–36.
[21] Hassan AHA, Kurgan N. Modeling and buckling analysis of rectangular plates in ANSYS. Int J Eng Appl Sci 2019;11:310–29.
[22] Van den Boom S. Topology optimisation including buckling analysis [Master Thesis]. Delft University of Technology; 2014.
[23] Reddy JN. An introduction to the finite element method, vol. 27. McGraw-Hill Book Company, New York; 1993.
[24] Stegmann J, Lund E. Discrete material optimization of general composite shell structures. Int J Numer Methods Eng 2005;62:2009–27.